17th World Conference on Earthquake Engineering, 17WCEE
Sendai, Japan - September 13th to 18th 2020

EVALUATION OF ROTATION CAPACITY OF STEEL WIDE FLANGE MEMBERS SUBJECTED TO LATERAL CYCLIC LOADING

A. Mohabeddine [1], J.A.F.O. Correia [2], J.M. Castro [3]

(1) *Ph.D. student, Department of Civil Engineering, Faculty of Engineering University of Porto, amohabeddine@fe.up.pt*

(2) *Researcher and invited professor, INEGI & Department of Civil Engineering, Faculty of Engineering University of Porto, jacorreia@fe.up.pt*

(3) *Assistant professor, Department of Civil Engineering, Faculty of Engineering University of Porto, miguel.castro@fe.up.pt*

Abstract

In the context of performance-based earthquake engineering, the prediction of the inelastic deformation capacity of moment resisting frame members is of paramount interest. Plastic rotation limits are among the key parameters to define the different damage states at the component level, which are very important for the development of component-based vulnerability functions. With the emergence of seismic performance-based assessment/design in structural engineering practice, there is a need for the improvement of the codified rotation limits. Rotation limits are essential for modeling purposes as well as for design checks in nonlinear structural analysis. The provisions provided in Part 3 of Eurocode 8 (EC8-3) have been the subject of discussion in the literature. Important updates are expected to be implemented in the upcoming version of EC8-3. Based on advanced finite element analysis, this paper presents a study for the evaluation of rotation capacity-limits corresponding to different damage states for steel beams with profiles found in European steel construction practice. A robust finite element model was developed in ABAQUS to simulate the behavior of steel members subjected to cyclic bending inducing large plastic deformations. The numerical model was validated with experimental data. The model is able to capture reasonably well the behavior of steel members including the buckling modes observed experimentally. An extensive parametric study is conducted by considering different aspects such as the effect of material steel grades, geometrical imperfections, member length, and the dependence on local slenderness. Finally, empirical equations based on multivariate regression analysis are proposed for the evaluation of plastic rotations at pre-capping and 80% reduction of bending moment strength.

Keywords: steel beams, steel moment-resisting frames, cyclic, rotation capacity, damage state.

17th World Conference on Earthquake Engineering, 17WCEE
Sendai, Japan - September 13th to 18th 2020

1. Introduction

Within the performance-based earthquake engineering context, the prediction of accurate rotation capacity of steel beams is of paramount interest. The rotations obtained from cyclic testing are the key parameters to define the damage states that support the development of component-fragility curves that are in turn used for building specific loss assessment (Elkady *et al*. [1]). Besides, with the emergence of performance-based seismic assessment in design offices, the rotations are crucial for the development of the numerical model and represent the acceptance criteria for design checks. Recently, practicing engineers Bech *et al*. [2] raised some concerns regarding the inaccuracy of ASCE41-13[3] rotations provided for steel columns. In the European context, the provisions provided in Part 3 of Eucorode 8 (EC8-3)[4] related to the assessment of steel members subjected to flexural loading, have been the subject of a lot of discussion in the literature [5]–[7]. Major updates of the codified rotations are expected in the upcoming version of the EC8-3. This study aims to contribute to this issue by focusing on the characterization of the rotation capacity of steel beams with European profiles.

Lignos and Krawinkler [8] collected a large database of experimental results available in the literature that were performed for the characterization of the cyclic behavior of moment connections after the Northridge earthquake, where moment-resisting frames connections exhibited poor behaviour. The authors used the data of sub-assemblies that developed their plastic hinge in the beam and derived empirical equations to quantify the important parameters that affect the cyclic moment-rotation relationship of a steel beam such as the pre-capping and post-capping plastic rotations. The proposal of the aforementioned study is extensively used in the literature for the calibration of concentrated plasticity models used for nonlinear analysis. Observations on the data used in the aforementioned study revealed that the largest portion of the dataset includes sections that have beam depth between 0.5m and 1.0m, which is a typical cross-section range used in construction practice in the U.S. However, smaller sections are usually found in European practice [9]. The rotation capacity of a member depends on the combination of several parameters related to the geometrical and material characteristics of the structural member. The non-correspondence of profiles is unlikely to provide the best results when adopting Lignos and Krawinkler [8] rotation capacities for European profiles. An earlier study conducted by Kazantzi *et al*. [10] used the same approach to estimate the ultimate rotation capacity using tests on sub-assemblies with European profiles only. However, their proposal is limited due to the lack of experimental data available in the literature. Lately, the EqualJoints European research project (D'Aniello *et al*. [11], Tartaglia *et al*. [12]) made available more experimental data on moment connections subjected to cyclic loading that are of great interest to the scientific community.

Recently, an experimental campaign has focused on the issue of the quantification of the deformation capacity and over-strength of European steel members (D'Aniello *et al*. [9]). Isolated steel beams with I and H European profiles were tested under monotonic and cyclic loading. However, the results were limited in terms of the number of specimens and the size cross-section profiles used in testing. Therefore, Araujo *et al*. [5] conducted an extensive numerical study to cover a wider range of cross-sections. The authors proposed empirical equations to estimate the rotations for European profiles under monotonic and cyclic loading, for the revision of EC8-3. However, the FE model used for the simulations under cyclic loading had some shortcomings and limitations that influence the results. Firstly, the cyclic plasticity material model was calibrated in a simplified manner to fit the experimental moment-rotations curves of the steel beams, instead of using material coupon tests. The softening and hardening of the material model would be strongly dependent on the local geometrical instabilities that triggered strength degradation instead of the pure material behavior, which might lead to inaccurate response. Secondly, the geometrical imperfections that influence considerably the rotation capacity of the member were not considered in the model.

This paper presents an improved version of Araujo *et al*. [5] work that is developed within the same research group at the University of Porto. A robust finite element model validated with experimental data was developed to simulate bare steel beams under cyclic loading. The material plasticity model was calibrated using experimental data on cyclic coupon tests. A parametric study was conducted on steel beams subjected to cyclic loading considering different parameters such as the effect of member length, geometrical imperfections, and material steel grades. In this paper, the results obtained on steel beams with IPE profiles are presented.

17th World Conference on Earthquake Engineering, 17WCEE
Sendai, Japan - September 13th to 18th 2020

2. Definition of steel beam damage states

EC8-3 considers three damage states, namely: Damage limitation (DL), Significant Damage (SD), and Near Collapse (NC). The quantification of each damage state is expressed in terms of plastic rotation at the end member, as multiple of yield rotation "*θy"*. For example, for class 1 profiles, the ductility ratios of *1θy, 6θy, and 8θy* correspond to the aforementioned performance levels, in respective order. The code provisions require that at DL limit state, the beam should be fully operational after an earthquake event, only little material plastic deformations are allowed; at SD limit state, beams are supposed to develop their full plastic moment without geometrical instabilities; and at NC limit state, the member can experience geometrical instabilities such as local buckling. However, these requirements are not very clear, particularly, in the case of DL and SD damage states. Several experimental studies [13] reported flange buckling at very early stages of hardening without causing loss of bending strength. Therefore, the requirement of EC8-3 for DL and SD limits can be overlapping in this case. The free edge of the flange plate is very vulnerable to buckle under compression stresses. The requirement of SD limit states provided in EC8-3 (i.e. plastic deformations only, excluding local buckling) is difficult to quantify and penalizes significantly the level of rotation for steel beams that can sustain additional loads and plastic deformations. Therefore, in this study different assumptions are considered for the definition of the damage states. The requirements of the rotations at DL limit state can be very disputable, therefore it is beyond the scope of this study. Therefore, only SD and DL limits are considered in the parametric study. Based on the definitions provided in the literature [5], the rotation limit for SD limit state is considered as the plastic rotation at pre-capping "*θp*", which is the maximum rotation achieved by the member before strength degradation initiates. The rotation limit at NC is taken as "$\theta_{80\%}$" which is the plastic rotation at *80%* reduction of the maximum bending strength, after the initiation of strength degradation. After the NC limit state, the cyclic degradation continues to occur until collapse due to fracture. The rotation at collapse damage state is useful for collapse analysis. However, it is beyond the scope of this study. Extrapolation of the descending branch of the backbone curve might be considered as an option. The definitions of pre-capping rotation "*θp*" and the rotation at 80% reduction of maximum bending moment "$\theta_{80\%}$" are shown in Fig. 1.

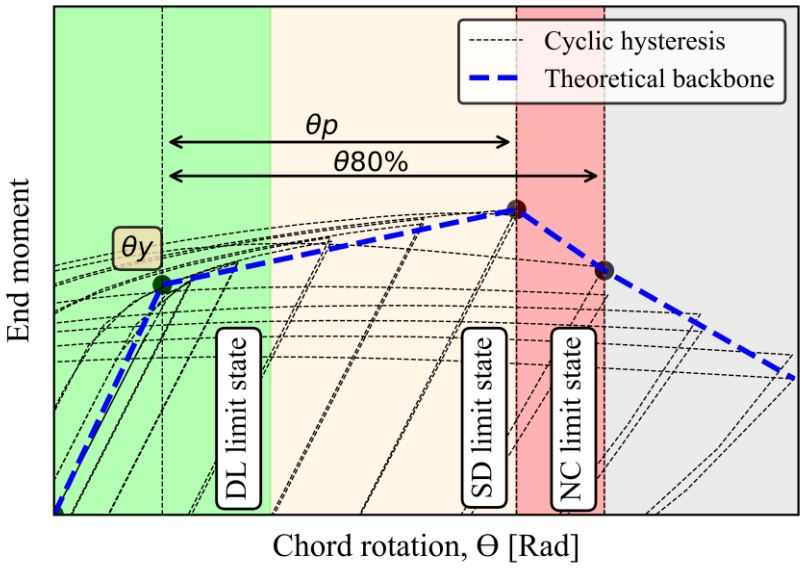

Fig. 1 - Definition of EC8-3 damage states.

3. Finite element model and validation

The finite element model was developed in the commercial software ABAQUS [14]. The model consists of a cantilever beam that was initially developed to simulate the tests conducted by D'Aniello *et al*. [9]. One edge of the cantilever was fully restrained in its 6 degrees of freedom to ensure fixed boundary conditions. The

cyclic loading was applied on the other edge of the beam in the strong axis of the section, as quasi-static displacement with amplitude history. This free-edge was restrained in the out-of-plane direction to avoid out-of-plane displacements, as in the experimental setup. The beam's plates were modeled using quadratic shell elements S4R, known to capture well large inelastic deformation and post-buckling behavior. After a mesh sensitivity study, the mesh size was taken equal to *bf/24*, where *bf* is the flange width. Lateral restraints were applied along the length of the beam to prevent lateral and torsional buckling. The distance between the lateral restraints was determined according to AISC 341-16 [15]. Flange and web imperfections are included in the model considering the manufacturer's shape tolerances provided in EN10034 [16]. The combined nonlinear kinematic and isotropic hardening material model was adopted to simulate the cyclic behavior of the material. The material model was calibrated using experimental data on coupons subjected to ascending and alternate cyclic loading protocols, provided by Chen et al [17], [18].

Fig. 2 compares the buckling failure modes observed in the F.E model and the once reported from the experimental program [9], for IPE300 and HEA160 beams. We can see that the F.E model captures reasonably well the buckling behavior, where, in Fig. 2 (a) IPE 300 beam experienced lateral and torsional buckling and in Fig. 2 (b) HEA 160 beams experienced anti-symmetric flange buckling accompanied with web local buckling. A comparison of the moment-chord rotation response between experimental and numerical results is shown in Fig. 3. Overall a good matching between experimental and numerical curves is achieved.

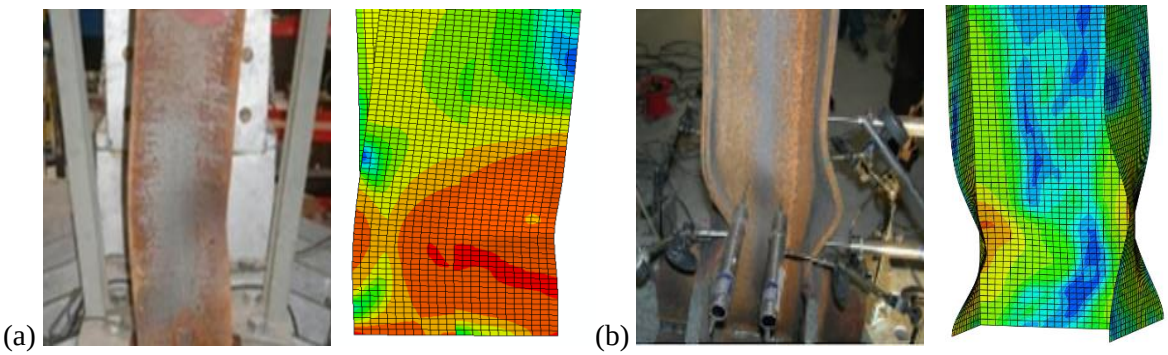

Fig. 2 - Comparison between experimental buckling modes on specimens tested under cyclic loading by D'Aniello et al. [9] and F.E results (a) IPE300; (b) HEA160.

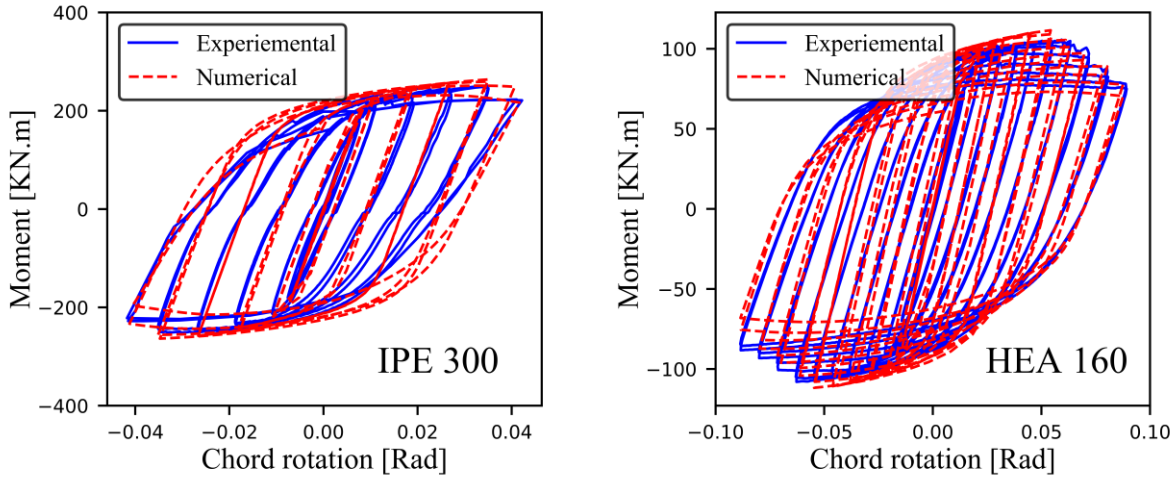

Fig. 3 - Comparison between experimental moment–chord rotations curves of IPE300 and HEA160 reported by D'Aniello et al. [9], and numerical predictions.

17th World Conference on Earthquake Engineering, 17WCEE
Sendai, Japan - September 13th to 18th 2020

4. Simulation program and loading protocol

A total of 238 simulations of bare steel beams subjected to lateral cyclic loading were performed in ABAQUS. This includes models with different profiles, member lengths, material steel grades, braced length, and geometrical imperfections. In this study, only a set of beams with IPE profiles is selected for discussion. The simulation program matrix is presented in Table 1.

Table 1: Simulation program matrix.

	L=2m	**L=3m**	**L=4m**	**L=6m**
S355	IPE200 ➔ 600	IPE200➔ 600	IPE300➔ 600	IPE400➔ 600
S235	IPE200 ➔ 600	-----	-----	-----

In this study, the SAC cyclic loading protocol [19] is adopted for all numerical simulations. This loading protocol is the most widely used in research for testing moment-resisting frames components. It is also adopted by seismic design codes such as AISC 341 [15]. Under cyclic loading, the failure of the beam depends strongly on the amplitude of the loading and the plastic deformations accumulated through the number of inelastic excursions imposed by the loading protocol. Therefore, it is important to mention that the results of this study are loading history-dependent and are limited to only one loading protocol. Recently, ATC 114 [20] discussed the use of less conservative loading protocol since an earthquake ground motion would generally subject structural components to a relatively fewer number of cycles with large amplitudes compared to the SAC protocol. However, the effect of different loading protocols is beyond the scope of this paper. The loading history applied in this work is presented in Fig. 4.

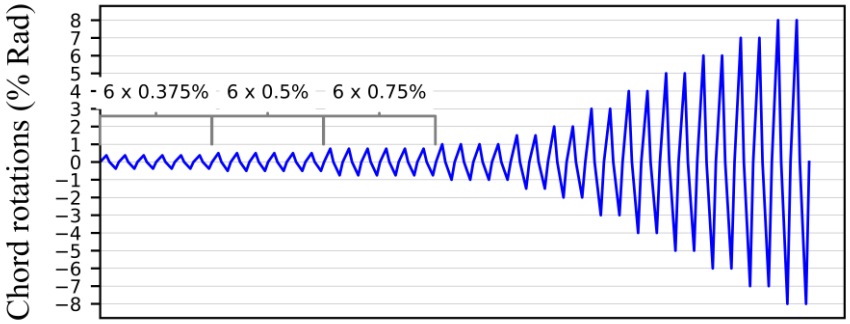

Fig. 4 - SAC cyclic loading protocol [19].

5. Results and discussion

Fig. 5 illustrates the variation trends of the plastic rotations $\theta 80\%$ with respect to the input parameters used for the regression model shown in Eq. (1) and Eq. (2). Fig. 5 (a) shows the dependence of the plastic rotations on the length-to-beam depth ratio "*L/h*" that is known to affect the flexural behavior of the beams. We can see that the rotations are proportional to *L/h*, which is in-line with previous experimental results [8]. Fig. 5 (b) compares the rotations of IPE beams (L=2m) with two steel grades, namely, S235 and S355. As expected, beams with S235 achieved higher plastic rotations. However, the comparison shows no significant difference. The higher material ductility of S235 steel over S355 observed in the experimental data [17], [18], seems to have a little influence on the plastic rotations for IPE beams. The possible explanation for this little influence of material ductility can be related to the strong dependence of the rotations on the web geometrical instability. Once the local buckling was triggered in the web, abrupt strength degradation began in the numerical model. Thus, the additional development of ductility due to material hardening does not appear in the response of the member. Fig. 5 (c) and (d) illustrate the dependence of the plastic rotations on the web slenderness "*h/tw*" and flange slenderness "*b/2tf*", respectively. Fig. 5 (c) reveals a clear dependence of the rotations on the ratio h/tw.

Where the plastic rotations at *θ80%* tend to decrease with increasing *h/tw*. In Fig. 5 (d), the influence of the flange slenderness ratio shows a lot of scattering of the results. However, a thorough analysis of the data showed that it is important to include *b/2tf* in the regression model since it supports for accounting the interaction between flange and web slenderness. We can observe the influence of "*b/2tf*" in the coefficient of the regression models shown in Eq. (1) and Eq. (2), where the coefficients have negative signs which means they are inversely proportional to the rotations.

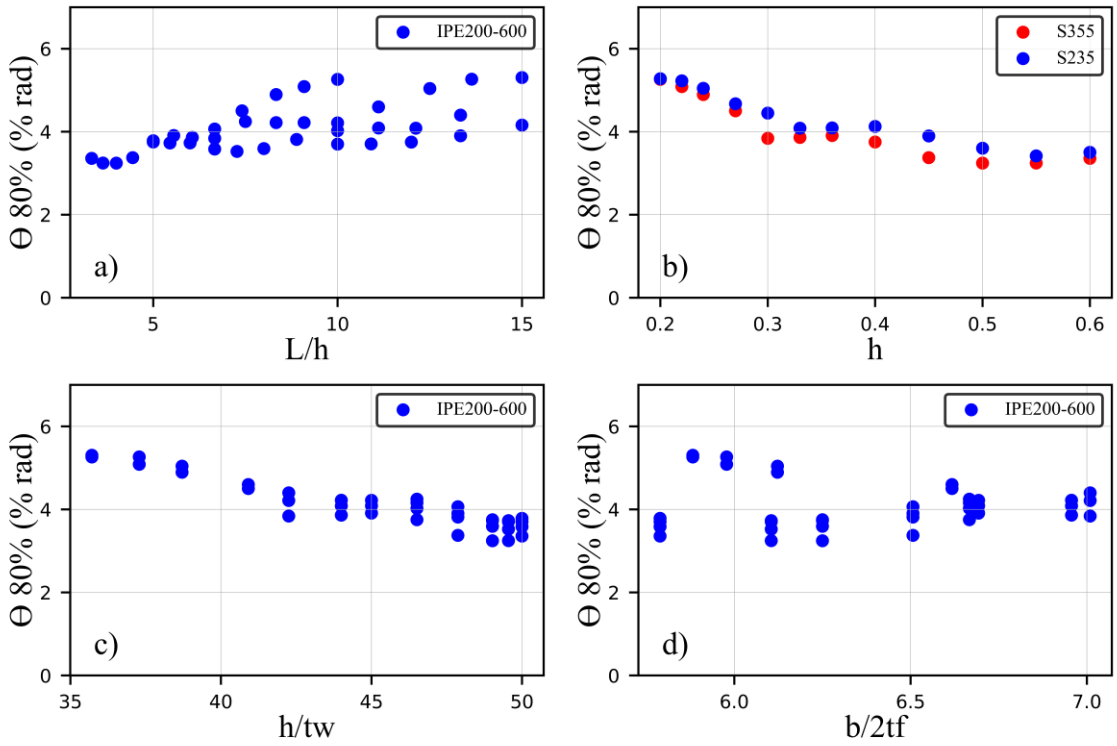

Fig. 5 – Variation trends of plastic rotations *θ80%* for IPE beams: (a) *θ80%* vs L/h; (b) *θ80%* vs beam depth "h" with beams of S235 and S355 steel grades; (c) *θ80%* vs h/tw; (d) *θ80%* vs b/2tf.

6. Regression expression for predicting rotations θ_P and $\theta_{80\%}$

In this section, empirical equations based on nonlinear regression analysis are proposed to predict the plastic rotations of steel beams with IPE profile subjected to cyclic loading. The input parameters included in the multivariate regression analysis are the once that are found to have a considerable influence on the response of the beam, as shown in section 5. This includes parameters related to the local slenderness of the member, member length, and material steel grade.

The pre-capping rotation θ_p can be estimated using Eq. (1), and the rotation at 80% of the maximum moment $\theta_{80\%}$ using Eq. (2). In these regression equations, more parameters (i.e. member length and material steel grade) are included in the regression analysis compared to the proposal of Araujo et al [5], where only local slenderness parameters were included in their equations.

$$\theta_p = 1.9388 \left(\frac{h}{t_w}\right)^{-0.1211} \left(\frac{b}{2t_f}\right)^{-1.104} \left(\frac{L}{h}\right)^{0.1309} \left(\frac{f_y}{355}\right)^{-0.3119} \quad (1)$$

$$\theta_{80\%} = 1.9313 \left(\frac{h}{t_w}\right)^{-0.1278} \left(\frac{b}{2t_f}\right)^{-1.007} \left(\frac{L}{h}\right)^{0.1003} \left(\frac{f_y}{355}\right)^{-0.1620} \quad (2)$$

17th World Conference on Earthquake Engineering, 17WCEE
Sendai, Japan - September 13th to 18th 2020

Where h: Section height
b: Flange width
t_w: Web thickness
t_f: Flange thickness
f_y: Length of the cantilever (note: in framed structures, the half shear span should be taken)
f_y: Yield stress in N/mm^2.

Fig. 5 depicts the fitting of Eq. (1) and Eq. (2) with the FE results for θ_p and $\theta_{80\%}$, respectively. The regression equations show the coefficient of determinations "R²" of 0.771 and 0.9351 for Eq. (1) and Eq. (2), respectively.

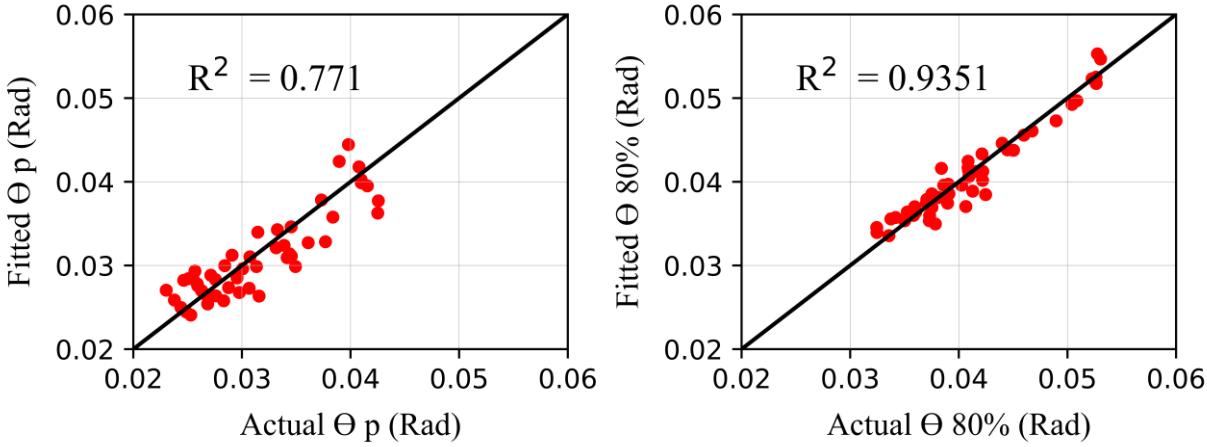

Fig 6 - Fitting of the nonlinear regression analysis.

7. Summary and future works

This paper presented a numerical study that focused on the evaluation of the rotation capacity of steel beams subjected to cyclic loading. The main findings and achievements of this work can be summarized as follows:

- A robust finite element model that can simulate the cyclic behavior steel beams was developed in ABAQUS. The model was validated with experimental data.
- A new definition for the Significant Damage damage state is was proposed.
- Plastic rotations of beams with IPE profiles are significantly influenced by the web slenderness.
- New empirical equations are proposed to estimate the plastic rotations for IPE steel members at pre-capping and at 80% reduction of maximum bending strength, which corresponds to SD and NC damage states.

Ongoing and futures works will involve:

- Further validation of the numerical model against experimental data.
- Incorporation of experimental results in the regression model.
- Characterization of the uncertainty due to geometrical imperfections.
- Inclusion of the influence of the lateral braced-length on the rotation capacity.

8. Acknowledgments

The authors would like to thank Dr. Mario D'Aniello from the University of Naples "Federico II" for providing the experimental results and steel beams and steel connections adopted in this study for comparison.

The authors would like also to thank Dr. Tak-Ming Chan from the Polytechnic University of Hong Kong for providing experimental data on material behavior used for the calibration of the plasticity cyclic model.

9. References

[1] A. Elkady, S. Ghimire, and D. G. Lignos, "Fragility curves for wide-flange steel columns and implications for building-specific earthquake-induced loss assessment," *Earthq. Spectra*, vol. 34, no. 3, pp. 1405–1429, 2018.

[2] Daniel Bech; Jonas Houston; Bill Tremayne, "ASCE 41-17 Steel Column Modeling and Acceptance Criteria," in *ASCE: Structures Congress 2017*, 2017, pp. 556–569.

[3] ASCE/SEI 41-13, *American Society of Civil Engineers : seismic evaluation and retrofit of existing buildings*. 2013.

[4] CEN, "Eurocode 8 : Design of structures for earthquake resistance-Part 3: Assessment and retrofitting of buildings." 2005.

[5] M. Araújo, L. Macedo, and J. M. Castro, "Evaluation of the rotation capacity limits of steel members defined in EC8-3," *J. Constr. Steel Res.*, vol. 135, no. April, pp. 11–29, 2017.

[6] H. El Jisr, A. Elkady, and D. G. Lignos, "Composite steel beam database for seismic design and performance assessment of composite-steel moment-resisting frame systems," *Bull. Earthq. Eng.*, vol. 17, no. 6, pp. 3015–3039, 2019.

[7] M. Araujo and J. Castro, "Deformation Capacity of Steel Members," in *EURO STEEL 2014*, 2014, no. September, pp. 1–10.

[8] D. G. Lignos, A. M. Asce, H. Krawinkler, and M. Asce, "Deterioration Modeling of Steel Components in Support of Collapse Prediction of Steel Moment Frames under Earthquake Loading," *J. Struct. Eng.*, vol. 137, no. 11, pp. 1291–1302, 2011.

[9] M. D 'Aniello, R. Landolfo, V. Piluso, and G. Rizzano, "Ultimate behavior of steel beams under non-uniform bending," *JCSR*, vol. 78, pp. 144–158, 2012.

[10] A. K. Kazantzi, T. D. Righiniotis, and M. K. Chryssanthopoulos, "The effect of joint ductility on the seismic fragility of a regular moment resisting steel frame designed to EC8 provisions," *J. Constr. Steel Res.*, vol. 64, no. 9, pp. 987–996, 2008.

[11] M. D'Aniello, R. Tartaglia, S. Costanzo, and R. Landolfo, "Seismic design of extended stiffened end-plate joints in the framework of Eurocodes," *J. Constr. Steel Res.*, vol. 128, pp. 512–527, 2017.

[12] R. Tartaglia, M. D'Aniello, G. A. Rassati, J. A. Swanson, and R. Landolfo, "Full strength extended stiffened end-plate joints: AISC vs recent European design criteria," *Eng. Struct.*, vol. 159, no. June 2017, pp. 155–171, 2018.

[13] R. D. Ziemian, *Guide To Stability Design Criteria for Metal*, JOHN WILEY. Hoboken, New Jersey, 2010.

[14] Dassault, "ABAQUS User's Manual," *ABAQUS/CAE User's Man.*, pp. 1–847, 2012.

[15] A. AISC 341-16, *Seismic Provisions for Structural Steel Buildings*, AMERICAN I. Chicago, 2016.

[16] British Standards, "BS EN 10034:1993 Structural steel I and H sections Tolerances on shape and dimensions," no. February 1993.

[17] Y. C. W. S. T.-M. Chan, "Effect of Loading Protocols on the Hysteresis Behaviour of Hot-Rolled Structural Steel with Yield Strength up to 420 MPa," *Adv. Struct. Eng. Vol.*, vol. 16, no. 4, pp. 707–719, 2013.

[18] Y. Chen, W. Sun, and T.-M. Chan, "Cyclic stress-strain behavior of structural steel with yield strength up to 460 N/mm2," *Front. Struct. Civ. Eng.*, vol. 8, no. 2, pp. 178–186, Jun. 2014.

[19] P. Clark, K. Frank, H. Krawinkler, and R. Shaw, "Protocol for Fabrication, Inspection, Testing, and Documentation of Beam-Column Connection Tests and Other Experimental Specimens," SAC Steel Project Background Document, Report No. SAC/BD-97/02," 1997.

[20] R. O. Hamburger *et al.*, "ATC-114 Next-Generation Hysteretic Relationships for Performance-based Modeling and Analysis."

